blood
Leading the world in reporting basic and applied hematology research
JOURNAL OF THE AMERICAN SOCIETY OF HEMATOLOGY
Original Article | Current Issue | About Blood | Submissions | Subscriptions | Contact Us

Blood. Nov 1, 2008; 112(9): 3867–3877. PMCID: PMC2572805
Prepublished online Aug 18, 2008. doi: 10.1182/blood-2007-11-126029
Phagocytes

FcγR-stimulated activation of the NADPH oxidase: phosphoinositide-binding protein p40^{phox} regulates NADPH oxidase activity after enzyme assembly on the phagosome

Wei Tian,[1,*] Xing Jun Li,[1,*] Natalie D. Stull,[1] Wenyu Ming,[1] Chang-Il Suh,[1] Sarah A. Bissonnette,[2] Michael B. Yaffe,[2,3,4] Sergio Grinstein,[5] Simon J. Atkinson,[6] and Mary C. Dinauer[1,7]

[1]Herman B Wells Center for Pediatric Research, Department of Pediatrics (Hematology/Oncology), Riley Hospital for Children, Indiana University School of Medicine, Indianapolis;
[2]Department of Biology and
[3]Division of Biological Engineering, Center for Cancer Research, Massachusetts Institute of Technology, Cambridge;
[4]Department of Surgery, Beth Israel Deaconess Medical Center, Boston, MA;
[5]Division of Cell Biology, Hospital for Sick Children, Toronto, ON; and
Departments of [6]Medicine (Nephrology) and
[7]Microbiology/Immunology and Medical and Molecular Genetics, Indiana University School of Medicine, Indianapolis
Corresponding author.
*W.T. and X.J.L. contributed equally to this work.

Received November 26, 2007; Accepted July 12, 2008.

Abstract

The phagocyte NADPH oxidase generates superoxide for microbial killing, and includes a membrane-bound flavocytochrome b_{558} and cytosolic p67^{phox}, p47^{phox}, and p40^{phox} subunits that undergo membrane translocation upon cellular activation. The function of p40^{phox}, which binds p67^{phox} in resting cells, is incompletely understood. Recent studies showed that phagocytosis-induced superoxide production is stimulated by p40^{phox} and its binding to phosphatidylinositol-3-phosphate (PI3P), a phosphoinositide enriched in membranes of internalized phagosomes. To better define the role of p40^{phox} in FcγR-induced oxidase activation, we used immunofluorescence and real-time imaging of FcγR-induced phagocytosis. YFP-tagged p67^{phox} and p40^{phox} translocated to granulocyte phagosomes before phagosome internalization and accumulation of a probe for PI3P. p67^{phox} and p47^{phox} accumulation on nascent and internalized phagosomes did not require p40^{phox} or PI3 kinase activity, although superoxide production before and after phagosome sealing was decreased by mutation of the p40^{phox} PI3P-binding domain or wortmannin. Translocation of p40^{phox} to nascent phagosomes required binding to p67^{phox} but not PI3P, although the loss of PI3P binding reduced p40^{phox} retention after phagosome internalization. We conclude that p40^{phox} functions primarily to regulate FcγR-induced NADPH oxidase activity rather than assembly, and stimulates superoxide production via a PI3P signal that increases after phagosome internalization.

Introduction

Phagocytic leukocytes are the front-line cellular defense against microbial attack, and are mobilized rapidly to the sites of infection where they ingest and kill opsonized microorganisms. The NADPH oxidase complex plays a central role in this process, as its assembly and activation on phagosomal membranes generate superoxide, the precursor of potent microbicidal oxidants. The importance of this

enzyme is demonstrated by genetic defects in the NADPH oxidase complex that cause chronic granulomatous disease (CGD), characterized by recurrent severe and potentially lethal bacterial and fungal infections.[1]

The NADPH oxidase includes the membrane-integrated flavocytochrome *b*, composed of gp91^{phox} and p22^{phox}, and the cytosolic components p47^{phox}, p67^{phox}, p40^{phox}, and Rac, a Rho-family GTPase, which translocate to flavocytochrome *b* upon cellular stimulation to activate superoxide production.[2–4] Segregation of regulatory components to the cytosol in resting cells facilitates the temporal and spatial regulation of NADPH oxidase activity. The p67^{phox} subunit is a Rac-GTP effector[2–4] containing a domain that activates electron transport through the flavocytochrome.[5] In resting cells, p67^{phox} is associated with p40^{phox} via complementary PB1 (phagocyte oxidase and Bem1p) motifs present in each protein.[2,6–8] p67^{phox} is also linked to p47^{phox} via a high-affinity interaction involving an SH3 domain and a proline-rich region, respectively, in the C-termini of these subunits.[2–4,6,9] The p67^{phox}, p47^{phox}, and p40^{phox} subunits can be isolated as a complex from neutrophil cytosol, and upon cellular activation, are believed to translocate as such to the flavocytochrome. p47^{phox} plays a key role as a carrier protein as the other 2 cytosolic *phox* proteins fail to undergo membrane translocation in p47^{phox}-deficient CGD neutrophils.[10–12] Translocation to the flavocytochrome is mediated by a pair of SH3 domains within p47^{phox} that are unmasked by activation-induced phosphorylation, which then bind to a proline-rich target sequence in p22^{phox}.[2–4,13]

The role of p40^{phox}, the most recently discovered NADPH oxidase subunit, has been controversial.[14] Mutations in p40^{phox} are not a cause of CGD,[1] and p40^{phox} is not required for high-level superoxide production in response to soluble agonists in either cell-free assays or whole-cell models.[14–16] In addition to the PB1 domain that mediates binding to p67^{phox}, p40^{phox} has a PX (*phox* homology) and an SH3 domain. The physiologic target of the p40^{phox} SH3 domain is uncertain, whereas the PX domain specifically binds phosphatidylinositol-3-phosphate (PI3P), which is enriched in early endosomes[17] and also appears on phagosomal membranes by the action of class III PI3 kinase (PI3K) within minutes of phagosome internalization in macrophages.[18–22]

Despite the importance of phagocytosis-induced superoxide production for host defense, the events regulating NADPH oxidase assembly and activation on the phagosome are incompletely defined. p47^{phox} and p67^{phox} are detected on the cup of newly forming phagosomes, and then on internalized phagosomes for many minutes after ingestion.[11,23,24] Oxidant production can also begin on the plasma membrane and continues after phagosome internalization.[4,25–27] Phagocytosis activates multiple signaling pathways, including PI3K's, although their specific roles are still being elucidated.[3,4,28–32] FcγR ligation induces activation of class I PI3Ks early in phagocytosis, which generate PI(3,4,5)P and PI(3,4)P on the phagosome cup, and class III PI3K, which produces PI3P on internalized phagosomes.[20] Following recognition that the PX domain of p40^{phox} binds to PI3P,[18–22] p40^{phox} was established as an important regulator of phagocytosis-induced superoxide production.[28,30,33,34] In COS^{phox} cells with transgenes for flavocytochrome *b*, p47^{phox}, p67^{phox}, and the FcγIIA receptor, NADPH oxidase activity induced by phagocytosis of IgG-opsonized targets required coexpression of p40^{phox}.[30] In addition, superoxide production in response to IgG-opsonized particles and *Staphylococcus aureus* was substantially reduced in neutrophils and PLB-985 granulocytes lacking p40^{phox},[28,34] and PI3P binding to p40^{phox} was essential to stimulate phagosomal oxidase activity in both neutrophils and COS^{phox} cells.[28,30] In both the COS^{phox} model and in permeabilized human neutrophils, mutants in the p40^{phox} PB1 and SH3 domains, especially the double mutation, also impaired p40^{phox} function, which suggests that binding of p40^{phox} to p67^{phox} as well as an additional target is required for regulation of FcγR-induced superoxide production.[28,30,34]

The underlying mechanism(s) by which p40^{phox} regulates phagocytosis-activated superoxide production is not fully understood. p40^{phox} has been proposed both to function as a second carrier

protein that mediates recruitment of $p67^{phox}$ to PI3P-rich phagosome membranes[29,35,36] and/or to regulate activity of the oxidase complex in combination with PI3P.[22,28,29,34,37] To better define the role of $p40^{phox}$ in superoxide production during phagocytosis, we examined the dynamics of FcγR-induced $p40^{phox}$ accumulation on phagosomes and its coordination with NADPH oxidase assembly and activation, using both the COS^{phox} model and videomicroscopy of PLB-985 neutrophils expressing fluorescently tagged *phox* subunits and/or the PX domain of $p40^{phox}$, a robust probe for PI3P.

Methods

Reagents

Sheep red blood cell (SRBC) and rabbit anti-SRBC IgG were from MP Biomedicals (Solon, OH). Rabbit polyclonal $p40^{phox}$ antibody was from Upstate Biotechnology (Lake Placid, NY), and $p67^{phox}$ and $p47^{phox}$ mAbs were from BD Biosciences (Franklin Lakes, NJ). pEYFP-C1, pEYFP-N1, pMSCVpuro, and puromycin were from BD Clontech (Franklin Lakes, NJ), and pSuper(neo) plasmid from Oligoengine (Seattle, WA). Cell line nucleofector Kit V and Kit T were from Amaxa (Gaithersburg, MD). Bovine growth serum (BGS) and fetal calf serum (FCS) were from HyClone Laboratory (Logan, UT). Other tissue culture materials, Alexa-conjugated antibodies, and Bioparticle Opsonizing Reagent were from Invitrogen Life Technologies (Carlsbad, CA). Hygromycin was from EMD Biosciences (San Diego, CA); G418, from Calbiochem (San Diego, CA); and ECL detection kit, from Pierce (Rockford, IL). Other reagents were from Sigma-Aldrich (St Louis, MO) unless stated.

Constructs for expression of fluorescence-tagged proteins

pEYFP-C1–based plasmids for expression of the YFP-tagged PX domain of $p40^{phox}$ (YFP-PX_{40}) or for YFP-$p40^{phox}$ and mutant derivatives were described.[21,30] Retroviral vectors to express YFP-$p40^{phox}$R105A, YFP-$p40^{phox}$W207R, and YFP-$p40^{phox}$D289A were generated by subcloning corresponding cDNAs into a modified pMSCVpuro lacking the PGK-puromycin cassette. A cDNA for $p67^{phox}$ tagged at its C-terminus with YFP was made using pEYFP-N1 and subcloned into pMSCVpac or derivative lacking the PGK-puromycin cassette. A cDNA encoding the $p40^{phox}$ PX domain with flanking *Eco*RI and *Kpn*I restriction sites was generated by polymerase chain reaction (PCR) of pEYFP-C1 containing YFP-PX_{40},[21] which was ligated to the mCherry cDNA[38] (gift of R. Tsien, University of California at San Diego) by insertion into a modified pEYFP-C1 (gift from J. Swanson, University of Michigan, Ann Arbor) in which the EYFP cDNA was replaced with that of mCherry. The mCherry-tagged PX_{40} cDNA was subcloned into pMSCVpuro and the PGK-puromycin cassette removed. Retroviral vectors were packaged using the Pantropic Retroviral Expression System (BD Clontech).

Cell lines and tissue culture

$p67^{phox}$-YFP–expressing COS7 cell lines were made from COS7 cells expressing $gp91^{phox}$, $p22^{phox}$, $p47^{phox}$, and FcγIIA receptor, in the presence or absence of a transgene for $p40^{phox}$,[16,30] by transducing with MSCV-p67YFP and sorting for YFP (FACSVantage; BD Biosciences). The 2 cell lines, called COSPF-p67YFP and COSPF40-p67YFP (PF = Phox FcγIIA), were cultured as described.[30] Media for COSPF-p67YFP cells contained 0.2 mg/mL hygromycin, 0.8 mg/mL neomycin, and 1 μg/mL puromycin. Blasticidin (10 μg/mL) was included for COSPF40-p67YFP cells. Wild-type COS7 cells expressing a transgenic FcγIIA receptor (COS-WF cells) were described.[30]

PLB-985 cells expressing YFP-$p40^{phox}$[30] were transduced with MSCV-Cherry-PX_{40} to generate a derivative coexpressing Cherry-PX_{40}. PLB-985 cells expressing fluorescently tagged $p67^{phox}$ or $p40^{phox}$ mutants were generated by transduction with MSCVpac-p67YFP, MSCV-YFP-$p40^{phox}$R105A, MSCV-YFP-$p40^{phox}$W207R, or MSCV-YFP-$p40^{phox}$D289A. The latter 3 were sorted by flow cytometry, whereas the former was selected in puromycin. PLB-985 lines were cultured and induced for neutrophil differentiation as described.[39] To examine effects on translocation, pEYFP-C1 plasmids for

expression of YFP-tagged $p40^{phox}$ mutants[30] were transfected into neutrophil-differentiated PLB-985 cells with Amaxa Nucleofector kit T and program Y-01[40] and incubated at 37°C for 3 hours before study.

Generation of $p40^{phox}$-deficient PLB-985 cells

Integrated DNA Technologies (IDT, Coralville, IA) online program was used to design shRNA sequences targeting the human $p40^{phox}$ transcript: 546*GGCAGCTCCGAGAGCAGAGGCTCTATT*572 (H1), 69*GGCCAACATTGCTGACATCGAGGAGAA*95 (H2), and 684*GGGCATCTTCCCTCTCTCCTTCGTGAA*710 (H3). *Bgl*II and *Hin*dIII sites were added to each end of the hairpin. After ligation into pSuper(neo), each recombinant plasmid, or empty vector, was transfected into PLB-p67YFP cells using Amaxa nucleofector Kit V and program-23. Clones were selected with 1.5 mg/mL G418 and screened by Western blot for $p40^{phox}$ expression after neutrophil differentiation. Two of 6 clones selected for expression of the H3 shRNA showed a significant decrease in $p40^{phox}$, and were used in described experiments. G418-selected PLB-p67YFP cells transfected with the empty pSuper(neo) vector were used as controls.

A pLL3.7-derived lentivirus carrying a hairpin targeting a 3′ untranslated sequence in the endogenous $p40^{phox}$ transcript, 5′-TGGAGATTGGGACCAGGAAATTCAAGAGATTTCCTGGTCCCAATCTCCTTTTTTC-3′,[34] was used to transduce PLB-985, PLB-YFPp40, and PLB-YFPp40R105A cells and clones selected in 2 μg/mL puromycin. Two of 10 selected clones for each line showed a substantial decrease in endogenous $p40^{phox}$ expression in neutrophil-differentiated cells, and were used in experiments.

Western blotting

Triton X-100 lysates from COS7 or neutrophil-differentiated PLB-985 cells were prepared for electrophoresis and Western blots as described.[16,30,41] In some experiments, the Triton X-100–insoluble pellet was also analyzed by electrophoresis and Western blotting as described.[42]

IgG-opsonized particles and assays for NADPH oxidase activity

SRBCs and 3.3-μm Latex beads were opsonized with human IgG as described.[30] Zymosan A particles were opsonized with either Bioparticle Opsonizing Reagent (rabbit anti–zymosan IgG) according the manufacturer's instructions or with human IgG at 20 mg/mL at 37° for 60 minutes. Final stock solutions were prepared at 20 mg/mL in PBS and stored at −20°C until use.

NADPH oxidase activity was assayed using chemiluminescence enhanced by luminol or isoluminol, which is membrane-impermeant; both compounds detect superoxide in a peroxidase-dependent reaction.[43,44] PLB-985 cells (2.5-5 × 10^5) or COS7-derived cells (2.5 × 10^5) in PBSG (PBS plus 0.9 mM $CaCl_2$, 0.5 mM $MgCl_2$, 20 mM dextrose) in the presence of 50 μM isoluminol or 50 μM luminol, without or with superoxide dismutase (SOD; final concentration: 75 μg/mL), were preincubated at 37°C for 10 minutes. Horseradish peroxidase (HRP; final concentration: 20 U/mL) was added to isoluminol assays and to luminol assays of COS^{phox} lines. IgG-opsonized particles or phorbol myristate acetate (PMA, 300 ng/mL) was added to activate cells (final volume: 200 μL), and the relative light units (RLU) were monitored at 60- to 90-second intervals for up to 1 hour by the Long Kinetic module in an Lmax microplate luminometer from Molecular Devices (Sunnyvale, CA). Integrated RLU values were calculated by SOFTmax software (Molecular Devices). In some experiments, a synchronized phagocytosis protocol[45] was adapted for NADPH oxidase assays. Briefly, PLB-985 neutrophils in 200 μL PBSG were incubated on ice for 5 minutes in 50 μM isoluminol and 20 U/mL HRP or 50 μM luminol, 75 μg/mL SOD, and 2000 U/mL catalase, then 25 μL cold IgG-zymosan (final concentration: 400 μg/mL) or cold IgG-Latex beads (cell:beads = 1:8) were added. Cells and particles were spun at 240*g* for 5 minutes at 4°C, then immediately placed at 37°C in the luminometer. For some experiments,

cells were preincubated for 30 minutes at 37°C in the presence or absence of 100 nM wortmannin.

Immunofluorescence microscopy

COSPF-p67YFP, COSPF40-p67YFP, and COS7-WF cells were plated into coverslip-bottomed dishes (MatTek Cultureware, Ashland, MA) and incubated at 37°C for 24 hours, washed with fresh media, loaded with IgG-SRBCs prelabeled with goat Alexa-633 anti–rabbit IgG, incubated for 15 minutes at 37°C, and washed with cold PBS. After distilled water lysis of external SRBCs, cells were fixed with 4% paraformaldehyde for 30 minutes. Samples were permeabilized with 0.2% Triton X-100 in PBS, blocked with 10% goat serum plus 2% BSA in PBS, and immunostained with anti-$p47^{phox}$ followed by Alexa-555 goat anti–mouse IgG. Nuclei were stained with 5 μg/mL DAPI in PBS for 5 minutes. Slides were imaged on a Zeiss LSM-510 confocal microscope (Carl Zeiss, Jena, Germany) using a 100×/1.4 NA oil-immersion objective. Samples were scanned sequentially at each excitation wavelength to minimize crosstalk between signals. Zeiss LSM software (Carl Zeiss) was used for image handling. Images shown are representative of at least 3 independent experiments.

Live cell imaging

A spinning-disk confocal system mounted on a Nikon TE-2000U inverted microscope (Nikon, Melville, NY) with an Ixon air-cooled EMCCD camera (Andor Technology, South Windsor, CT) and 100×/1.4 NA objective was used to film phagocytosis in living PLB-985 cells. Differentiated PLB-985 cells were loaded onto coverslip-bottomed dishes, which were mounted on the microscope and maintained at 37°C using a stage incubator (Warner Instruments, Hamden, CT). After 3 minutes, IgG-zymosan was loaded into the dish. Videos were made over an approximately 30-minute interval after the addition of IgG-zymosan. Fields were monitored randomly to identify cells beginning to ingest a particle, and sequential images collected with 488 nm and/or 568 nm excitation and 0.3-second exposure with a time lapse of 5 or 10 seconds for 5 to 8 minutes. Phagosomes being filmed often moved out of the focal plane, so a new cell beginning to ingest a particle was identified for filming. MetaMorph (Universal Imaging, Downington, PA) was used for image handling. Images shown are representative of at least 4 independent experiments except for studies on PLB-985 neutrophils transiently expressing YFP-$p40^{phox}$W207R or YFP-$p40^{phox}$D289A, which were performed 2 and 3 times, respectively.

To further assess translocation of fluorescent probes, images were analyzed using Image J (National Institutes of Health [NIH], Bethesda, MD). An area of the phagosome rim (≈ 25% of the total rim) was outlined by hand, and the mean fluorescence intensity within the area determined, and ratios were determined against the value from a corresponding area in the cytoplasm near the phagosome. At least 5 phagosomes monitored at each stage—cup, closure (time of sealing), and after internalization (200-300 seconds after closure, or 120 seconds after closure for YFP-$p40^{phox}$ R105A and for wortmannin-treated cells)—were analyzed by this method and the mean plus or minus SEM was determined.

Results

Recruitment of $p67^{phox}$ and $p47^{phox}$ to phagosomes is independent of $p40^{phox}$ in COS^{phox} cells

We examined whether expression of $p40^{phox}$ is required for recruitment of $p67^{phox}$ and $p47^{phox}$ to phagosomes in the COS^{phox} model. To facilitate imaging, COS7 cells were generated that stably expressed $p67^{phox}$-YFP along with $gp91^{phox}$, $p22^{phox}$, $p47^{phox}$, and the FcγIIA receptor, without or with coexpression of $p40^{phox}$ (Figure 1A). Previous studies showed that $p67^{phox}$ tagged in this manner supports NADPH oxidase activity at levels similar to untagged $p67^{phox}$.[23] In NADPH oxidase assays using luminol-enhanced chemiluminescence, although both lines responded similarly to PMA stimulation (Figure S1, available on the *Blood* website; see the Supplemental Materials link at the top of the online article), there was very little IgG-SRBC–stimulated superoxide in the absence of $p40^{phox}$ (Figure 1B,C), confirming our previous study.[30]

Next, the fate of p67^{phox}-YFP was monitored by confocal microscopy in COSPF-p67YFP and COSPF40-p67YFP cells incubated with IgG-SRBCs. The results showed that p67^{phox}-YFP was present on phagosomes in both COSPF-p67YFP and COSPF40-p67YFP cells (Figure 2). Indirect immunofluorescence showed that p47^{phox} colocalized with p67^{phox}-YFP on phagosomes in both cell lines (Figure 2B; Figure S2), consistent with the concept that p47^{phox} and p67^{phox} are tightly linked via a tail-to-tail interaction and translocate as a unit.[2,6,9,46] No p47^{phox} staining was observed in control COS-WF cells (Figure S2). These data indicate that although FcγR-activated superoxide production has a strong requirement for p40^{phox} in COS^{phox} cells, the absence of p40^{phox} does not prevent phagosomal translocation of p47^{phox} and p67^{phox}.

NADPH oxidase activation and translocation of p67^{phox}-YFP and YFP-p40^{phox} during phagocytosis in PLB-985 neutrophils

Assembly and activation of the NADPH oxidase complex was studied in neutrophil-differentiated PLB-985 cells expressing YFP-p40^{phox} (PLB-YFPp40) or p67^{phox}-YFP (PLB-p67YFP). Endogenous and YFP-tagged subunits were expressed at comparable levels (Figure 3A and data not shown). IgG-zymosan–induced NADPH oxidase activity in PLB-p67YFP neutrophils was assayed where particles were bound to cells at 4°C followed by warming to 37°C to initiate phagocytosis. Superoxide production began before sealing of phagosomes, as detected by isoluminol-enhanced chemiluminescence (Figure 3 B,C), although the magnitude of this response is small in comparison to extracellular superoxide detected following fMLP (not shown) or PMA (Figure S3A) stimulation. Peak rates of superoxide release occurred within minutes of warming, then declined to lower levels. NADPH oxidase activity in internalized phagosomes was detected using luminol in the presence of SOD and catalase (Figure 3D,E), with peak rates shifted in time compared with isoluminol. IgG-zymosan–induced NADPH oxidase activity both before and after phagosome internalization was substantially decreased by 100 nM wortmannin (Figure 3B-D). Of note, wortmannin had no effect on the ability of PLB-985 neutrophils to ingest IgG-zymosan particles (average of 1.9 phagosomes per cell in 50 to 65 cells analyzed in videos of untreated and wortmannin-treated cells). IgG-zymosan–stimulated superoxide production and wortmannin sensitivity of parental PLB-985 cells and PLB-YFPp40 were similar to PLB-p67YFP cells (not shown). Finally, as previously reported by many groups (eg, Arcaro and Wymann[47]; Laudanna et al[48]), wortmannin had no effect on PMA-induced NADPH oxidase activity (Figure S3B).

Time-lapse confocal videomicroscopy was used to monitor recruitment of YFP-p40^{phox} and p67^{phox}-YFP to phagosomes during ingestion of IgG-zymosan by PLB-985 neutrophils (Figure 4A,B; Videos S1,S2). Both p67^{phox}-YFP and YFP-p40^{phox}, which were otherwise distributed homogenously in the cytoplasm, accumulated on the phagosomal cup, visible 40 to 60 seconds before phagosome closure (sealing), and probes remained detectable on phagosomes for at least 5 minutes after closure. Accumulation of fluorescently tagged *phox* subunits often appeared nonuniform and/or “clumpy” (Figures 4–7 and Videos S1–S8). Although superoxide production was strongly dependent on PI3K activity (Figure 3B), wortmannin did not prevent recruitment of either p67^{phox}-YFP or YFP-p40^{phox} to nascent phagosomes (Figure 4C,D; Videos S3,S4). Interestingly, although p67^{phox}-YFP accumulation persisted after internalization, we observed that p40^{phox}-YFP accumulation disappeared in 2 of 7 phagosomes within 2 minutes after sealing, leading to a decline in average fluorescence intensity of the p40^{phox}-YFP probe (Figure 4D).

NADPH oxidase assembly and activation on phagosomes were next analyzed in p40^{phox}-deficient PLB-p67YFP cells generated using a p40^{phox}-targeted shRNA. Western blotting showed a substantial decrease in p40^{phox} and a small reduction in endogenous p67^{phox}, similar to previous studies in p40^{phox}-deficient mouse neutrophils,[28] but expression of YFP-tagged p67^{phox} appeared to be unaffected (Figure 5A). Similar to previous studies,[28,33,34] superoxide production in internalized phagosomes was reduced by approximately 2-fold in p40^{phox}-deficient PLB-p67YFP cells stimulated with either IgG-zymosan (Figure 5D,E) or IgG-opsonized Latex beads (not shown). Superoxide

production before phagosome sealing was also reduced by approximately 40% (Figure 5B,C). However, $p67^{phox}$-YFP accumulated on the phagosomal cup in $p40^{phox}$-deficient PLB-p67YFP cells and persisted for at least 5 minutes after closure (Figure 5F; Video S5), similar to PLB-p67YFP cells that express endogenous $p40^{phox}$ (Figure 4A). The independence of $p67^{phox}$-YFP translocation on $p40^{phox}$ is consistent with our findings in COS^{phox} cells (Figure 2), and supports a model in which translocation of $p67^{phox}$ to nascent and internalized phagosomes does not require $p40^{phox}$.

Role of PI3P and the PX, SH3, and PB1 domains of $p40^{phox}$ in FcγR-induced $p40^{phox}$ translocation to phagosomes

The appearance of YFP-$p40^{phox}$ in the phagosomal cup before the expected accumulation of phagosomal PI3P, which in macrophages occurs after phagosome internalization,[18–20] and its insensitivity to wortmannin suggested that the initial recruitment of $p40^{phox}$ to phagosomes does not require binding to PI3P. To directly examine the temporal relationship between the appearance of $p40^{phox}$ and PI3P on neutrophil phagosomes, phagocytosis was analyzed in PLB-YFPp40 neutrophils coexpressing the $p40^{phox}$ PX domain (PX_{40}), a probe for PI3P,[18] tagged with mCherry. Although YFP-$p40^{phox}$ was detected on the phagosomal cup, Cherry-PX_{40} did not accumulate until 40 to 60 seconds after the phagosome was sealed and internalized (Figure 6A; Videos S6,S7). Preincubation of cells in 100 nM wortmannin abolished accumulation of Cherry-PX_{40}, consistent with a requirement for PI3K to generate PI3P,[18,19] but YFP-$p40^{phox}$ was still present on many phagosomes (Figure 6B). These results further establish that recruitment of $p40^{phox}$ is not mediated by PI3P.

The role of each of the 3 $p40^{phox}$ modular domains in translocation to phagosomes was examined by expressing YFP-tagged $p40^{phox}$ mutants (Figure 7A) in PLB-985 neutrophils. These included a PX domain mutant, R105A, that eliminates binding to PI3P, the SH3 domain mutant W207R, and a PB1 domain mutant, D289A, that prevents binding of $p40^{phox}$ to $p67^{phox}$.[2,30,49,50] The $p40^{phox}$D289A mutant was poorly expressed from a stable transgene in PLB-985 granulocytes, most likely because binding to $p67^{phox}$ is important for $p40^{phox}$ stability in neutrophils, as inferred from studies of $p67^{phox}$-deficient CGD neutrophils which have markedly reduced levels of $p40^{phox}$[14]; $p40^{phox}$W207R was also poorly expressed in PLB-985 granulocytes, for uncertain reasons (Figure S4). Thus, we used a transient expression protocol developed for neutrophils[40] to study translocation of W207R, D289A, and a double W207R/D289A $p40^{phox}$ mutant in comparison with wild-type $p40^{phox}$. Translocation of $p40^{phox}$R105A was studied both as a transiently expressed protein and as expressed from a stable transgene, with similar results. Note that although an R57Q PI3P-binding mutant of $p40^{phox}$ was enriched in the Triton X-100–insoluble fraction,[42] this was not observed for $p40^{phox}$R105A (Figure S4).

Imaging by confocal videomicroscopy showed that R105A and W207R YFP-$p40^{phox}$ mutants were recruited to the phagosomal cup, similar to wild-type YFP-$p40^{phox}$ (Figure 7B,C). In contrast, YFP-$p40^{phox}$ derivatives with a mutation that prevents binding to $p67^{phox}$, D289A, and W207R/D289A YFP-$p40^{phox}$ were rarely detected on phagosomes, either before or after phagosome closure (Figure 7B and data not shown). For example, D289A YFP-$p40^{phox}$ translocation was seen in only 2 of 30 phagosomes analyzed. Wild-type YPP-$p40^{phox}$ and W207R YFP-$p40^{phox}$ were present on internalized phagosomes, similar to previous observations in the COS^{phox} model.[30] However, although the PI3P-binding mutant R105A YFP-$p40^{phox}$ appeared on nascent phagosomes, it often disappeared within minutes after closure (Figure 7B-D). In phagosomes followed from time of cup formation, R105A YFP-$p40^{phox}$ was present on only approximately one third of internalized phagosomes for longer than 3 minutes after sealing, in contrast to wild-type YFP-$p40^{phox}$ ($P < .03$; Fisher exact test; Figure 7D). In contrast, a similar analysis in $p40^{phox}$-deficient PLB-p67YFP cells found that $p67^{phox}$-YFP was detected on 11 of 11 phagosomes monitored for at least 3 minutes after phagosome closure (see also Figure 5F; Video S5). These data indicate that the PB1 domain–mediated interaction between $p40^{phox}$ and $p67^{phox}$ is required for recruitment of $p40^{phox}$, but not $p67^{phox}$, to both nascent and internalized

phagosomes, even with an intact binding site for PI3P in $p40^{phox}$. However, $p40^{phox}$ binding to PI3P appears to partially influence whether $p40^{phox}$ is present on phagosomal membranes after internalization. This effect is more pronounced compared with wortmannin treatment, which may reflect an influence of other wortmannin-inhibited pathways.

Role of the $p40^{phox}$ PX domain in FcγR-induced NADPH oxidase activity

To examine how loss of PI3P binding by $p40^{phox}$ affects NADPH oxidase activity, PLB-985, PLB-YFPp40, or PLB-YFPp40R105A cells were made deficient in endogenous $p40^{phox}$ using an shRNA targeting the 3′ untranslated region[34] (Figure 7E). As in a previous study using this shRNA,[34] $p67^{phox}$ expression in neutrophil-differentiated $p40^{phox}$ knockdown (p40KD) PLB-985 lines was similar to PLB-985 cells (Figure 7E). PMA-induced superoxide release in p40KD PLB-985 cells was robust and similar to p40KD PLB-985 cells expressing YFP-$p40^{phox}$ or YFP-$p40^{phox}$R105A. However, IgG-particle–activated superoxide production both before and after phagosome internalization was decreased by at least 40% in p40KD cells and p40KD cells expressing YFP-$p40^{phox}$R105A, compared with p40KD cells expressing YFP-$p40^{phox}$ (Figure 7F). Indeed, expression of YFP-$p40^{phox}$R105A tended to decrease activity to a greater extent than p40KD alone, suggestive of an inhibitory effect. Similar to studies in PLB-985 cells (Figure 7B-D), the R105A mutation did not prevent $p40^{phox}$ translocation to nascent phagosomes in p40KD cells (Video S8), consistent with the concept that although PI3P binding to $p40^{phox}$ stimulates enzyme activity, it is not required for initial $p40^{phox}$ translocation. However, as in Figure 7B-D, YFP-p40R105A often disappeared from internalized phagosomes in p40KD cells; of 8 phagosomes analyzed from time of cup formation, YFP-p40R105A was present on only 3 for longer than 3 minutes (see also Video S8).

Discussion

PI3Ks products play important roles in regulating superoxide production during phagocytosis, particularly PI3P that is enriched in membranes of internalized phagosomes and whose effects on NADPH oxidase activity are mediated via $p40^{phox}$.[28–30,33,34] The current study used real-time imaging of phagocytosis of IgG-opsonized particles to analyze assembly of the NADPH oxidase complex in neutrophil-differentiated PLB-985 cells. Particular emphasis was given to investigating the recruitment of the cytosolic NADPH oxidase subunits, $p40^{phox}$ and $p67^{phox}$, and the relationship between their translocation, the accumulation of PI3P, and superoxide production, to better characterize the role of $p40^{phox}$, which has high-affinity binding domains for both $p67^{phox}$ and PI3P.

This study confirms previous reports that $p67^{phox}$ is recruited to nascent granulocyte phagosomes and is present after internalization,[11,23,51] and shows for the first time that $p40^{phox}$ translocation during phagocytosis exhibits similar behavior and fails to accumulate on phagosomes if unable to bind to $p67^{phox}$. Conversely, $p40^{phox}$ was not required for accumulation of $p67^{phox}$ and $p47^{phox}$ on IgG-zymosan phagosomes in COS^{phox} cells expressing FcγIIA, although NADPH oxidase activity was minimal unless $p40^{phox}$ was coexpressed. Translocation of $p67^{phox}$ on nascent and internalized phagosomes was also observed in $p40^{phox}$-deficient PLB-985 neutrophils. Furthermore, $p67^{phox}$ and $p40^{phox}$ accumulated on nascent phagosomes before the appearance of a PI3P probe, and in the presence of the PI3K inhibitor wortmannin, indicating that PI3P binding to $p40^{phox}$ is dispensable for the initial recruitment of $p67^{phox}$ and $p40^{phox}$. Taken together, although confirming the importance of $p40^{phox}$ for phagocytosis-induced oxidant production, our results do not support a model in which PI3P-bound $p40^{phox}$ plays a significant role as a second carrier protein for $p67^{phox}$ to the phagosome, in addition to $p47^{phox}$. Although a recent study in arachidonic acid–stimulated RAW 267.4 macrophage cells showed that PI3P-dependent binding of $p40^{phox}$ can mediate recruitment of $p67^{phox}$ to early endosomes,[35] this setting is likely to have differences with phagocytic receptor–induced recruitment.

The current studies also reveal new insights into FcγR-induced $p40^{phox}$ recruitment to granulocyte phagosomes and the relative roles of its PI3P- and $p67^{phox}$-binding domains. Simultaneous imaging of fluorescently tagged probes determined that full-length $p40^{phox}$ translocated to the phagosomal cup, whereas accumulation of the $p40^{phox}$ PX domain, a probe for PI3P, occurred 40 to 60 seconds after phagosome sealing, kinetics similar to PI3P probes in macrophages.[18,19] Neither inhibition of PI3K by wortmannin nor an R105A mutation in $p40^{phox}$ that prevents PI3P binding eliminated recruitment of full-length $p40^{phox}$ to the phagosomal cup. However, a $p40^{phox}$ D289A mutation that disrupts its binding to $p67^{phox}$ almost completely abolished IgG-zymosan–induced translocation of $p40^{phox}$ in PLB-985 neutrophils, similar to the COS^{phox} model.[30] The importance of the PB1 domain for $p40^{phox}$ translocation in response to a physiologic signal extends results in a K562 cell model stimulated with either PMA or a muscarinic receptor[50] and in a PMA-stimulated permeabilized human neutrophil system.[34,37] Taken together, our data indicate that translocation of $p40^{phox}$ to both nascent and PI3P-rich internalized phagosomes is dependent on $p67^{phox}$ and does not initially require binding to PI3P. However, both wortmannin, and to an even greater extent, an R105A PI3P-binding mutant affected the persistence of $p40^{phox}$ on internalized phagosomes.

Our results support a model in which $p40^{phox}$, $p67^{phox}$, and $p47^{phox}$, linked by separate high-affinity binding sites in $p67^{phox}$ for $p47^{phox}$ and for $p40^{phox}$, translocate as a trimeric complex to the membrane-integrated flavocytochrome *b* after activation-induced unmasking of the $p47^{phox}$-binding site for $p22^{phox}$.[2–4,37,52–55] This model is consistent with studies in CGD patients lacking either flavocytochrome *b* or $p47^{phox}$ showing that stable translocation of the trimeric *phox* complex requires interactions between $p47^{phox}$ and flavocytochrome *b*.[10–12] For example, neither $p67^{phox}$ nor $p40^{phox}$ undergoes membrane translocation in $p47^{phox}$-deficient CGD neutrophils, whereas $p47^{phox}$ translocation is unaffected in $p67^{phox}$-deficient CGD.[10–12] Taken together, these data suggest that $p47^{phox}$ is necessary and sufficient for stable recruitment of $p67^{phox}$ to the flavocytochrome *b* in phagosomal membranes, which in turn mediates that of $p40^{phox}$.

A second implication from our results is that recruitment of cytosolic *phox* subunits of the NADPH oxidase complex to the phagosome is insufficient for high-level superoxide production, and the predominant role of PI3P binding by $p40^{phox}$ is to stimulate FcγR-induced superoxide production after enzyme assembly rather than to drive $p67^{phox}$ translocation. Whereas wild-type $p40^{phox}$ rescued phagocytosis-induced superoxide production in $p40^{phox}$-deficient PLB-985 neutrophils phagosomes, the R105A PX domain mutant did not, confirming previous studies[30,33] and extending these findings to show that an intact PI3P-binding domain is also required before sealing. This suggests that there may be small amounts of PI3P in the plasma membrane not detectable by imaging probes, as previously postulated,[28,33] and that the marked increase in PI3P on internalized phagosomes may function to up-regulate oxidase activity in this sequestered compartment. In addition, since $p40^{phox}$R105A is present in phagosomal cup, these results further establish a role for this domain apart from one in translocation. That PI3P-bound $p40^{phox}$ has a direct effect on the assembled enzyme is supported by studies in semirecombinant systems in which $p40^{phox}$ stimulates superoxide production in the presence of PI3P,[22,37] and where PI3P binding by the $p40^{phox}$ PX domain is required for oxidase activation but not for subunit translocation in vitro.[34] Finally, a comparison of FcγR-induced oxidase activity in wortmannin-treated PLB-985 cells with cells expressing $p40^{phox}$R105A suggests that a substantial portion of the wortmannin effect both before and after internalization is mediated through inhibition of PI3P production, again confirming and extending a study in murine neutrophils expressing a PI3P-binding $p40^{phox}$ mutant.[33]

The R105A PX domain mutant of $p40^{phox}$, which is unable to bind to PI3P, was recruited to nascent phagosomes but often disappeared within a few minutes after internalization. Why the PB1 domain–mediated interaction between $p67^{phox}$ and $p40^{phox}$, which is necessary for $p40^{phox}$ translocation to the phagosome, appears insufficient to maintain $p40^{phox}$R105A after internalization is a paradox that

will require further investigation. This observation also suggests that protein-protein interactions between oxidase subunits may be dynamic and are modified after assembly of the NADPH oxidase complex. In the resting state, the ability of the $p40^{phox}$ PX domain to access PI3P in the membrane is masked by an intramolecular interaction with the $p40^{phox}$ PB1 domain on the face opposite of the region that binds to $p67^{phox}$.[56] The mechanism that disrupts the intramolecular $p40^{phox}$ PX-PB1 interaction, leading to exposure of the PI3P-binding site, is unknown, although it does not appear to involve $p40^{phox}$ phosphorylation.[35,56] It is possible that conformational changes in $p40^{phox}$ that accompany the unmasking of its PX domain or other events after phagosome internalization result in a requirement for PI3P binding in order for $p40^{phox}$ to be retained on phagosomes. A role for PI3P in $p40^{phox}$ retention after phagosome internalization may contribute to reduced NADPH oxidase activity in cells expressing a PI3P-binding mutant of $p40^{phox}$.

In summary, this study demonstrates that membrane translocation of $p40^{phox}$ during FcγR-induced phagocyte NADPH oxidase assembly begins in the phagosomal cup and requires binding to $p67^{phox}$. The data are consistent with a model in which $p47^{phox}$ functions as the key adaptor protein that is necessary and sufficient to recruit $p67^{phox}$ and $p40^{phox}$ to the membrane-bound flavocytochrome *b*. Although $p40^{phox}$ is not required to mediate assembly of the other cytosolic *phox* subunits on the phagosome, $p40^{phox}$ stimulates activity of the assembled NADPH oxidase complex via a PI3P signal that is spatially and temporally regulated to increase on internalized phagosomes. Future challenges include identifying underlying mechanisms by which the PX domain in $p40^{phox}$ becomes accessible to PI3P, how PI3P influences localization of $p40^{phox}$ after phagosome closure, and how $p40^{phox}$ stimulates activity of the NADPH oxidase complex. For example, it is possible that PI3P-bound $p40^{phox}$ induces conformational changes in other NADPH oxidase subunits, or acts to tether the oxidase complex to an optimal membrane microdomain, as recent studies in a cell-free model system suggest that the membrane phospholipid environment can have a large influence on the activity of the assembled oxidase complex.[57]

Supplementary Material

[Supplemental Figures and Videos]

Acknowledgments

We thank Georges Marchal for construction of retroviral vectors for expression of YFP-tagged $p67^{phox}$, Christophe Marchal for assistance with analyzing $p40^{phox}$-shRNA–transduced PLB-985 clones, and Shari Upchurch and Melody Warman for assistance with paper preparation.

This work was supported by National Institutes of Health (Bethesda, MD) grants R01 HL45635 (M.C.D. and S.J.A.) and GM52981 (M.B.Y.), the Indiana University Cancer Center Flow Cytometry and Imaging Cores P30 CA082709, the Canadian Institutes for Health Research (Canadian IHR, Ottawa, ON; S.G.), and the Riley Children's Foundation (Indianapolis, IN; M.C.D.). Microscope facilities in the Indiana Center for Biological Microscopy are also supported by a grant (INGEN) from the Lilly Endowment (Indianapolis, IN).

Footnotes

The online version of this article contains a data supplement.

Presented in abstract form at the 48th Annual Meeting of the American Society of Hematology, Orlando, FL, December 11, 2006.[58]

The publication costs of this article were defrayed in part by page charge payment. Therefore, and solely to indicate this fact, this article is hereby marked “advertisement” in accordance with 18 USC section 1734.

Authorship

Contribution: W.T. and X.J.L. designed, performed, and analyzed experiments, prepared the figures, and helped draft the paper; W.M. and N.D.S. performed and analyzed experiments; C.-I.S. prepared critical reagents; S.A.B. and M.B.Y. provided a critical reagent; S.G. helped with interpretation of data and paper preparation; S.J.A. and M.B.Y. analyzed and interpreted data and helped with paper preparation; and M.C.D. oversaw this entire project including the experimental design, analysis, interpretation of the data, and preparation of the paper.

Conflict-of-interest disclosure: The authors declare no competing financial interests.

Correspondence: Mary C. Dinauer, Cancer Research Institute, R4 402C, Indiana University School of Medicine, 1044 W Walnut Street, Indianapolis, IN 46202; e-mail: mdinauer@iupui.edu.

References

1. Dinauer M. The phagocyte system and disorders of granulopoiesis and granulocyte function. In: Nathan DG, Orkin SH, Ginsburg D, Look AT, editors. Nathan and Oski's Hematology of Infancy and Childhood. 6th ed. Vol 1. Philadelphia, PA: WB Saunders Company; 2003. pp. 923–1010.

2. Groemping Y, Rittinger K. Activation and assembly of the NADPH oxidase: a structural perspective. Biochem J. 2005;386:401–416. [PMCID: PMC1134858] [PubMed: 15588255]

3. Quinn MT, Gauss KA. Structure and regulation of the neutrophil respiratory burst oxidase: comparison with nonphagocyte oxidases. J Leukoc Biol. 2004;76:760–781. [PubMed: 15240752]

4. Nauseef WM. Assembly of the phagocyte NADPH oxidase. Histochem Cell Biol. 2004;122:277–291. [PubMed: 15293055]

5. Nisimoto Y, Motalebi S, Han CH, Lambeth JD. The $p67^{phox}$ activation domain regulates electron flow from NADPH to flavin in flavocytochrome b_{558}. J Biol Chem. 1999;274:22999–23005. [PubMed: 10438466]

6. Lapouge K, Smith SJ, Groemping Y, Rittinger K. Architecture of the p40-p47-$p67^{phox}$ complex in the resting state of the NADPH oxidase: a central role for $p67^{phox}$. J Biol Chem. 2002;277:10121–10128. [PubMed: 11796733]

7. Tsunawaki S, Kagara S, Yoshikawa K, Yoshida LS, Kuratsuji T, Namiki H. Involvement of $p40^{phox}$ in activation of phagocyte NADPH oxidase through association of its carboxyl-terminal, but not its amino-terminal, with $p67^{phox}$. J Exp Med. 1996;184:893–902. [PMCID: PMC2192801] [PubMed: 9064349]

8. Wientjes FB, Panayotou G, Reeves E, Segal AW. Interactions between cytosolic components of the NADPH oxidase: $p40^{phox}$ interacts with both $p67^{phox}$ and $p47^{phox}$. Biochem J. 1996;317(pt 3):919–924. [PMCID: PMC1217573] [PubMed: 8760383]

9. Massenet C, Chenavas S, Cohen-Addad C, et al. Effects of $p47^{phox}$ C terminus phosphorylations on binding interactions with $p40^{phox}$ and $p67^{phox}$: structural and functional comparison of $p40^{phox}$ and $p67^{phox}$ SH3 domains. J Biol Chem. 2005;280:13752–13761. [PubMed: 15657040]

10. Dusi S, Della Bianca V, Donini M, Nadalini KA, Rossi F. Mechanisms of stimulation of the respiratory burst by TNF in nonadherent neutrophils: its independence of lipidic transmembrane signaling and dependence on protein tyrosine phosphorylation and cytoskeleton. J Immunol. 1996;157:4615–4623. [PubMed: 8906841]

11. Allen LA, DeLeo FR, Gallois A, Toyoshima S, Suzuki K, Nauseef WM. Transient association of the nicotinamide adenine dinucleotide phosphate oxidase subunits $p47^{phox}$ and $p67^{phox}$ with phagosomes

in neutrophils from patients with X-linked chronic granulomatous disease. Blood. 1999;93:3521–3530. [PubMed: 10233905]

12. Heyworth PG, Curnutte JT, Nauseef WM, et al. Neutrophil nicotinamide adenine dinucleotide phosphate oxidase assembly: translocation of $p47^{phox}$ and $p67^{phox}$ requires interaction between $p47^{phox}$ and cytochrome b_{558}. J Clin Invest. 1991;87:352–356. [PMCID: PMC295061] [PubMed: 1985107]

13. Groemping Y, Lapouge K, Smerdon SJ, Rittinger K. Molecular basis of phosphorylation-induced activation of the NADPH oxidase. Cell. 2003;113:343–355. [PubMed: 12732142]

14. Matute JD, Arias AA, Dinauer MC, Patino PJ. $p40^{phox}$: the last NADPH oxidase subunit. Blood Cells Mol Dis. 2005;35:291–302. [PubMed: 16102984]

15. de Mendez I, Leto TL. Functional reconstitution of the phagocyte NADPH oxidase by transfection of its multiple components in a heterologous system. Blood. 1995;85:1104–1110. [PubMed: 7849298]

16. Price MO, McPhail LC, Lambeth JD, Han CH, Knaus UG, Dinauer MC. Creation of a genetic system for analysis of the phagocyte respiratory burst: high-level reconstitution of the NADPH oxidase in a nonhematopoietic system. Blood. 2002;99:2653–2661. [PubMed: 11929750]

17. Gillooly DJ, Morrow IC, Lindsay M, et al. Localization of phosphatidylinositol 3-phosphate in yeast and mammalian cells. EMBO J. 2000;19:4577–4588. [PMCID: PMC302054] [PubMed: 10970851]

18. Ellson CD, Anderson KE, Morgan G, et al. Phosphatidylinositol 3-phosphate is generated in phagosomal membranes. Curr Biol. 2001;11:1631–1635. [PubMed: 11676926]

19. Vieira OV, Botelho RJ, Rameh L, et al. Distinct roles of class I and class III phosphatidylinositol 3-kinases in phagosome formation and maturation. J Cell Biol. 2001;155:19–25. [PMCID: PMC2150784] [PubMed: 11581283]

20. Yeung T, Ozdamar B, Paroutis P, Grinstein S. Lipid metabolism and dynamics during phagocytosis. Curr Opin Cell Biol. 2006;18:429–437. [PubMed: 16781133]

21. Kanai F, Liu H, Field SJ, et al. The PX domains of $p47^{phox}$ and $p40^{phox}$ bind to lipid products of PI(3)K. Nat Cell Biol. 2001;3:675–678. [PubMed: 11433300]

22. Ellson CD, Gobert-Gosse S, Anderson KE, et al. PtdIns(3)P regulates the neutrophil oxidase complex by binding to the PX domain of $p40^{phox}$. Nat Cell Biol. 2001;3:679–682. [PubMed: 11433301]

23. van Bruggen R, Anthony E, Fernandez-Borja M, Roos D. Continuous translocation of Rac2 and the NADPH oxidase component $p67^{phox}$ during phagocytosis. J Biol Chem. 2004;279:9097–9102. [PubMed: 14623873]

24. Ueyama T, Lennartz MR, Noda Y, et al. Superoxide production at phagosomal cup/phagosome through beta I protein kinase C during FcγR-mediated phagocytosis in microglia. J Immunol. 2004;173:4582–4589. [PubMed: 15383592]

25. Robinson JM, Ohira T, Badwey JA. Regulation of the NADPH-oxidase complex of phagocytic leukocytes: recent insights from structural biology, molecular genetics, and microscopy. Histochem Cell Biol. 2004;122:293–304. [PubMed: 15365846]

26. Ohno Y, Hirai K, Kanoh T, Uchino H, Ogawa K. Subcellular localization of H_2O_2 production in human neutrophils stimulated with particles and an effect of cytochalasin-B on the cells. Blood. 1982;60:253–260. [PubMed: 7082841]

27. Badwey J, Curnutte J, Robinson J, et al. Comparative aspects of oxidative metabolism of neutrophils from human blood and guinea pig peritonea: magnitude of the respiratory burst,

dependence upon stimulating agents, and localization of the oxidases. J Cell Physiol. 1980;105:541–551. [PubMed: 6257739]

28. Ellson CD, Davidson K, Ferguson GJ, O'Connor R, Stephens LR, Hawkins PT. Neutrophils from $p40^{phox-/-}$ mice exhibit severe defects in NADPH oxidase regulation and oxidant-dependent bacterial killing. J Exp Med. 2006;203:1927–1937. [PMCID: PMC2118373] [PubMed: 16880254]

29. Perisic O, Wilson MI, Karathanassis D, et al. The role of phosphoinositides and phosphorylation in regulation of NADPH oxidase. Adv Enzyme Regul. 2004;44:279–298. [PubMed: 15581496]

30. Suh CI, Stull ND, Li XJ, et al. The phosphoinositide-binding protein $p40^{phox}$ activates the NADPH oxidase during FcγIIA receptor-induced phagocytosis. J Exp Med. 2006;203:1915–1925. [PMCID: PMC2118377] [PubMed: 16880255]

31. Lee JS, Nauseef WM, Moeenrezakhanlou A, et al. Monocyte p110α phosphatidylinositol 3-kinase regulates phagocytosis, the phagocyte oxidase, and cytokine production. J Leukoc Biol. 2007;81:1548–1561. [PubMed: 17369495]

32. Baggiolini M, Dewald B, Schnyder J, Ruch W, Cooper PH, Payne TG. Inhibition of the phagocytosis-induced respiratory burst by the fungal metabolite wortmannin and some analogues. Exp Cell Res. 1987;169:408–418. [PubMed: 3556425]

33. Ellson C, Davidson K, Anderson K, Stephens LR, Hawkins PT. PtdIns3P binding to the PX domain of $p40^{phox}$ is a physiological signal in NADPH oxidase activation. EMBO J. 2006;25:4468–4478. [PMCID: PMC1589987] [PubMed: 16990793]

34. Bissonnette SA, Glazier CM, Stewart MQ, Brown GE, Ellson CD, Yaffe MB. Phosphatidylinositol 3-phosphate-dependent and -independent functions of $p40^{phox}$ in activation of the neutrophil NADPH oxidase. J Biol Chem. 2008;283:2108–2119. [PMCID: PMC2755574] [PubMed: 18029359]

35. Ueyama T, Tatsuno T, Kawasaki T, et al. A regulated adaptor function of $p40^{phox}$: distinct $p67^{phox}$ membrane targeting by $p40^{phox}$ and by $p47^{phox}$. Mol Biol Cell. 2007;18:441–454. [PMCID: PMC1783789] [PubMed: 17122360]

36. Wientjes FB, Segal AW. PX domain takes shape. Curr Opin Hematol. 2003;10:2–7. [PubMed: 12483105]

37. Brown GE, Stewart MQ, Liu H, Ha VL, Yaffe MB. A novel assay system implicates PtdIns(3,4)P(2), PtdIns(3)P, and PKC delta in intracellular production of reactive oxygen species by the NADPH oxidase. Mol Cell. 2003;11:35–47. [PubMed: 12535519]

38. Shaner NC, Campbell RE, Steinbach PA, Giepmans BN, Palmer AE, Tsien RY. Improved monomeric red, orange and yellow fluorescent proteins derived from Discosoma sp. red fluorescent protein. Nat Biotechnol. 2004;22:1567–1572. [PubMed: 15558047]

39. Zhen L, King AA, Xiao Y, Chanock SJ, Orkin SH, Dinauer MC. Gene targeting of X chromosome-linked chronic granulomatous disease locus in a human myeloid leukemia cell line and rescue by expression of recombinant $gp91^{phox}$. Proc Natl Acad Sci U S A. 1993;90:9832–9836. [PMCID: PMC47666] [PubMed: 8234321]

40. Johnson JL, Ellis BA, Munafo DB, Brzezinska AA, Catz SD. Gene transfer and expression in human neutrophils. The phox homology domain of $p47^{phox}$ translocates to the plasma membrane but not to the membrane of mature phagosomes. BMC Immunol. 2006;7:28. http://www.biomedcentral.com/1471-2172/7/28. [PMCID: PMC1712351] [PubMed: 17150107]

41. Ming W, Li S, Billadeau DD, Quilliam LA, Dinauer MC. The Rac effector $p67^{phox}$ regulates phagocyte NADPH oxidase by stimulating Vav1 guanine nucleotide exchange activity. Mol Cell Biol.

2007;27:312–323. [PMCID: PMC1800642] [PubMed: 17060455]

42. Chen J, He R, Minshall RD, Dinauer MC, Ye RD. Characterization of a mutation in the phox homology domain of the NADPH oxidase component $p40^{phox}$ identifies a mechanism for negative regulation of superoxide production. J Biol Chem. 2007;282:30273–30284. [PubMed: 17698849]

43. Dahlgren C, Karlsson A. Respiratory burst in human neutrophils. J Immunol Methods. 1999;232:3–14. [PubMed: 10618505]

44. Lundqvist H, Dahlgren C. Isoluminol-enhanced chemiluminescence: a sensitive method to study the release of superoxide anion from human neutrophils. Free Radic Biol Med. 1996;20:785–792. [PubMed: 8728025]

45. Greenberg S, Burridge K, Silverstein SC. Colocalization of F-actin and talin during Fc receptor-mediated phagocytosis in mouse macrophages. J Exp Med. 1990;172:1853–1856. [PMCID: PMC2188739] [PubMed: 2124254]

46. Mizuki K, Takeya R, Kuribayashi F, et al. A region C-terminal to the proline-rich core of $p47^{phox}$ regulates activation of the phagocyte NADPH oxidase by interacting with the C-terminal SH3 domain of $p67^{phox}$. Arch Biochem Biophys. 2005;444:185–194. [PubMed: 16297854]

47. Arcaro A, Wymann MP. Wortmannin is a potent phosphatidylinositol 3-kinase inhibitor: the role of phosphatidylinositol 3,4,5-trisphosphate in neutrophil responses. Biochem J. 1993;296(pt 2):297–301. [PMCID: PMC1137693] [PubMed: 8257416]

48. Laudanna C, Rossi F, Berton G. Effect of inhibitors of distinct signalling pathways on neutrophil Q2- generation in response to tumor necrosis factor-alpha, and antibodies against CD18 and CD11a: evidence for a common and unique pattern of sensitivity to wortmannin and protein tyrosine kinase inhibitors. Biochem Biophys Res Commun. 1993;190:935–940. [PubMed: 8094958]

49. Bravo J, Karathanassis D, Pacold CM, et al. The crystal structure of the PX domain from $p40^{phox}$ bound to phosphatidylinositol 3-phosphate. Mol Cell. 2001;8:829–839. [PubMed: 11684018]

50. Kuribayashi F, Nunoi H, Wakamatsu K, et al. The adaptor protein $p40^{phox}$ as a positive regulator of the superoxide-producing phagocyte oxidase. EMBO J. 2002;21:6312–6320. [PMCID: PMC136946] [PubMed: 12456638]

51. DeLeo FR, Allen LA, Apicella M, Nauseef WM. NADPH oxidase activation and assembly during phagocytosis. J Immunol. 1999;163:6732–6740. [PubMed: 10586071]

52. Huang J, Kleinberg ME. Activation of the phagocyte NADPH oxidase protein $p47^{phox}$. Phosphorylation controls SH3 domain-dependent binding to $p22^{phox}$. J Biol Chem. 1999;274:19731–19737. [PubMed: 10391914]

53. Nobuhisa I, Takeya R, Ogura K, et al. Activation of the superoxide-producing phagocyte NADPH oxidase requires co-operation between the tandem SH3 domains of $p47^{phox}$ in recognition of a polyproline type II helix and an adjacent alpha-helix of $p22^{phox}$. Biochem J. 2006;396:183–192. [PMCID: PMC1449995] [PubMed: 16460309]

54. Ogura K, Nobuhisa I, Yuzawa S, et al. NMR solution structure of the tandem Src homology 3 domains of $p47^{phox}$ complexed with a $p22^{phox}$-derived proline-rich peptide. J Biol Chem. 2006;281:3660–3668. [PubMed: 16326715]

55. Sumimoto H, Hata K, Mizuki K, et al. Assembly and activation of the phagocyte NADPH oxidase. Specific interaction of the N-terminal Src homology 3 domain of $p47^{phox}$ with $p22^{phox}$ is required for activation of the NADPH oxidase. J Biol Chem. 1996;271:22152–22158. [PubMed: 8703027]

56. Honbou K, Minakami R, Yuzawa S, et al. Full-length $p40^{phox}$ structure suggests a basis for

regulation mechanism of its membrane binding. EMBO J. 2007;26:1176–1186. [PMCID: PMC1852833] [PubMed: 17290225]

57. Berdichevsky Y, Mizrahi A, Ugolev Y, Molshanski-Mor S, Pick E. Tripartite chimeras comprising functional domains derived from the cytosolic NADPH oxidase components $p47^{phox}$, $p67^{phox}$, and Rac1 elicit activator-independent superoxide production by phagocyte membranes: an essential role for anionic membrane phospholipids. J Biol Chem. 2007;282:22122–22139. [PubMed: 17548354]

58. Tian W, Li XJ, Stull ND, et al. The phosphoinositide-binding protein p40phox regulates NADPH oxidase activation rather than assembly during FcrIIA receptor-induced phagocytosis (abstract). Blood. 2006;108 Abstract 203a.

Figures and Tables

Figure 1

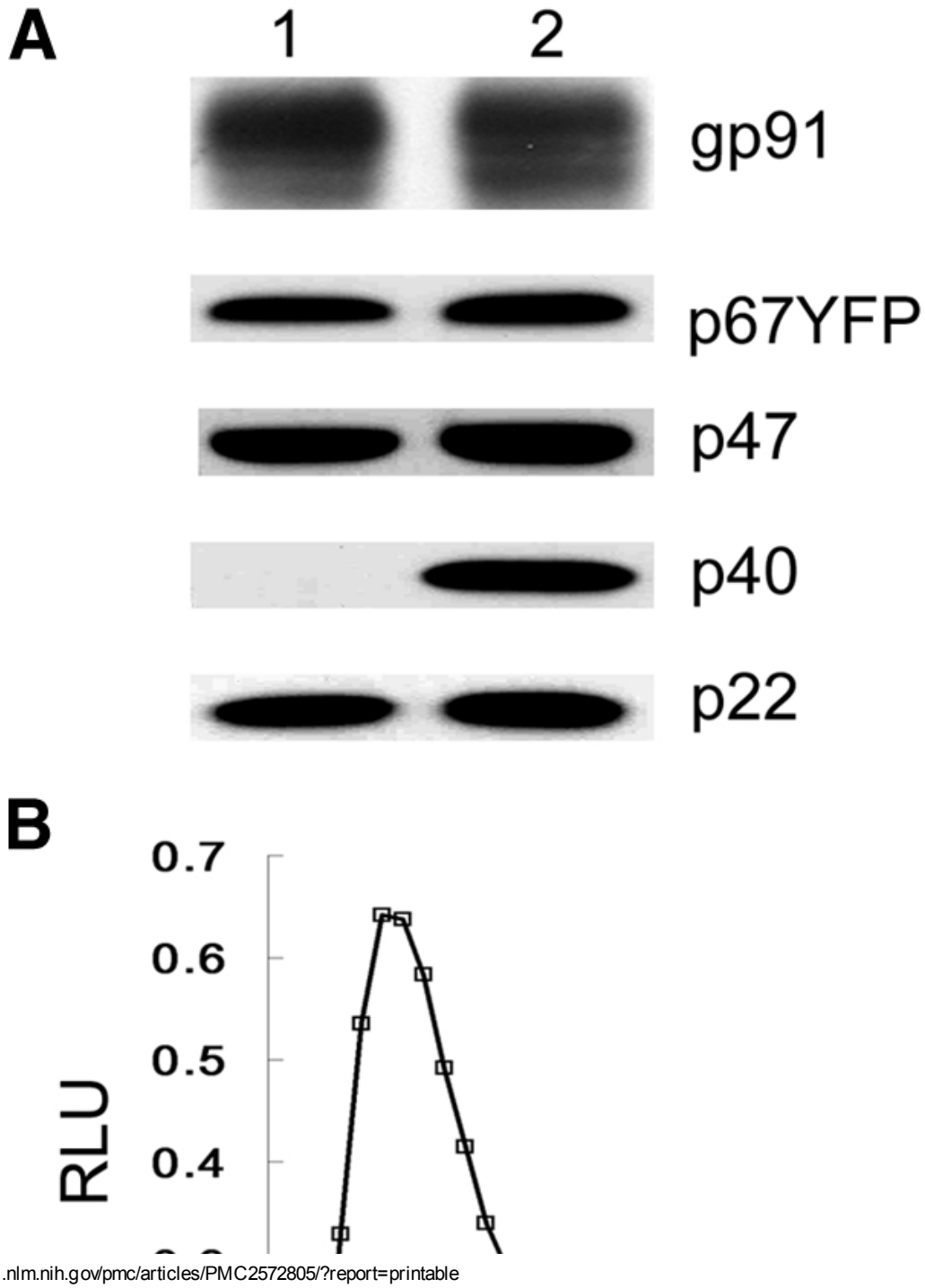

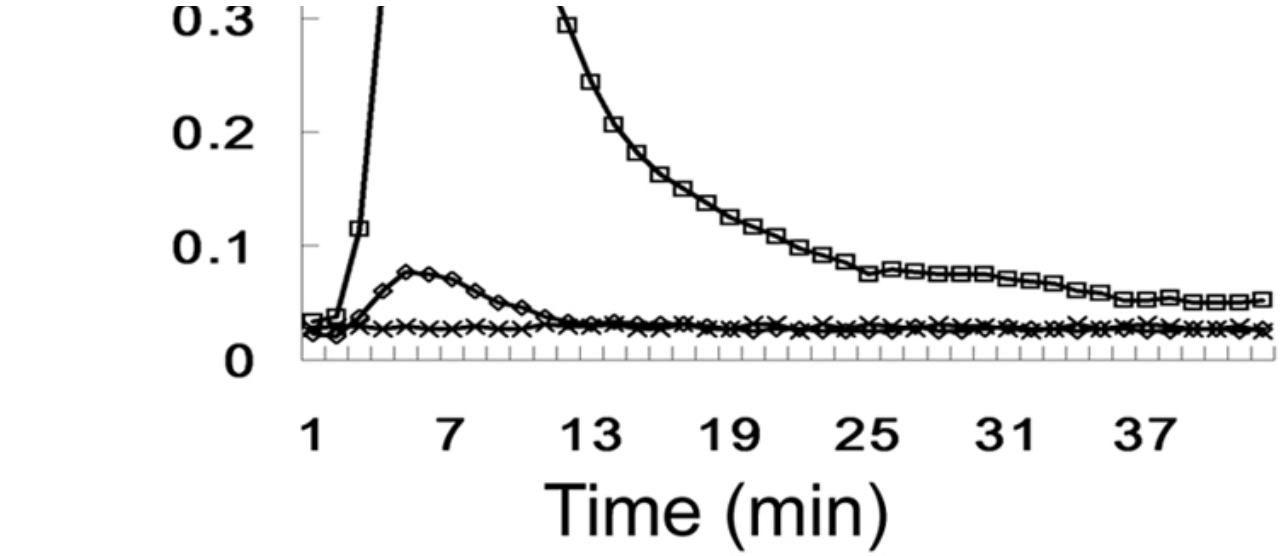

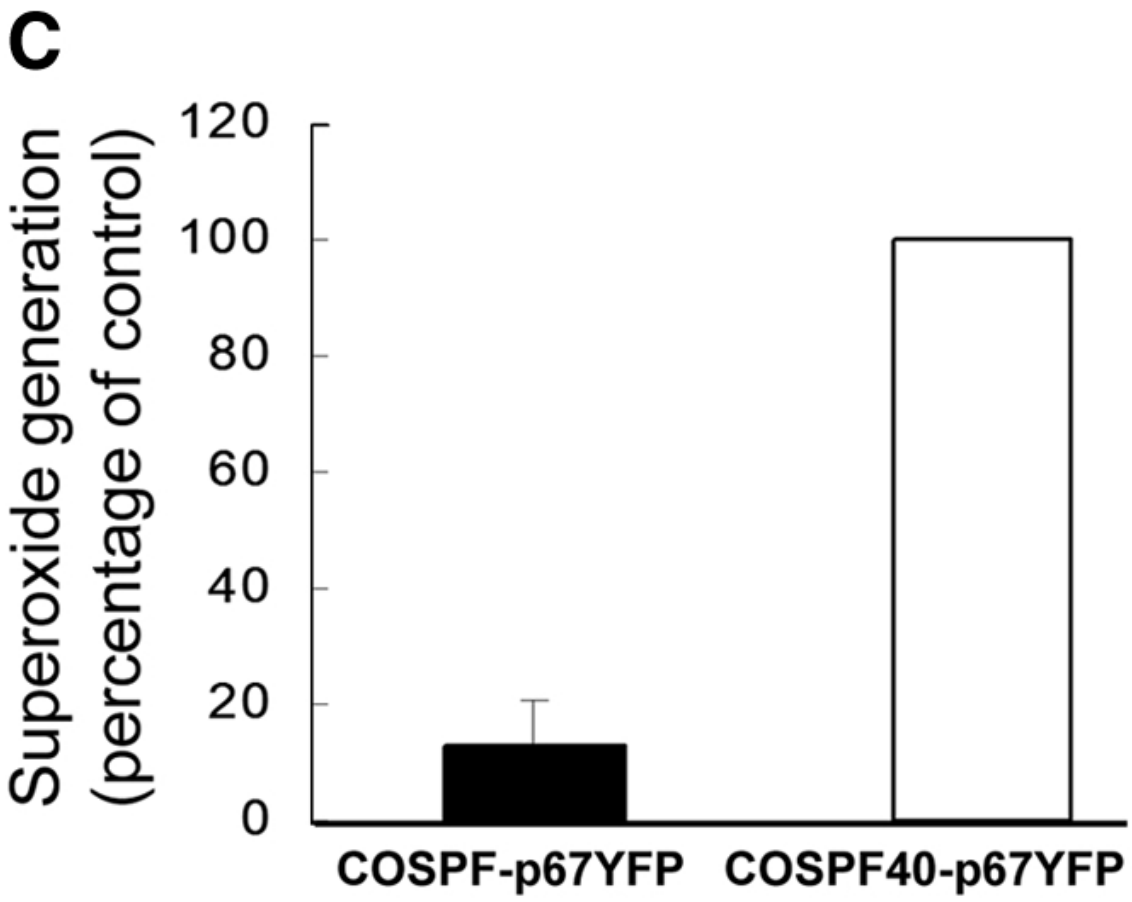

NADPH oxidase activity in COS7 transgenic cells. (A) Western blot analysis of COSPF-p67YFP (lane 1) and COSPF40-p67YFP (lane 2) cell lysates probed for expression of the indicated *phox* proteins. (B) Representative result of luminol assay for superoxide production in COS^{phox} cells during phagocytosis of IgG-opsonized SRBCs. □ indicates COSPF40-p67YFP; ◇, COSPF-p67YFP; and x, COS-WF. (C) Integrated RLU values for luminol assays of indicated cell lines (mean ± SD, n = 12).

Figure 2

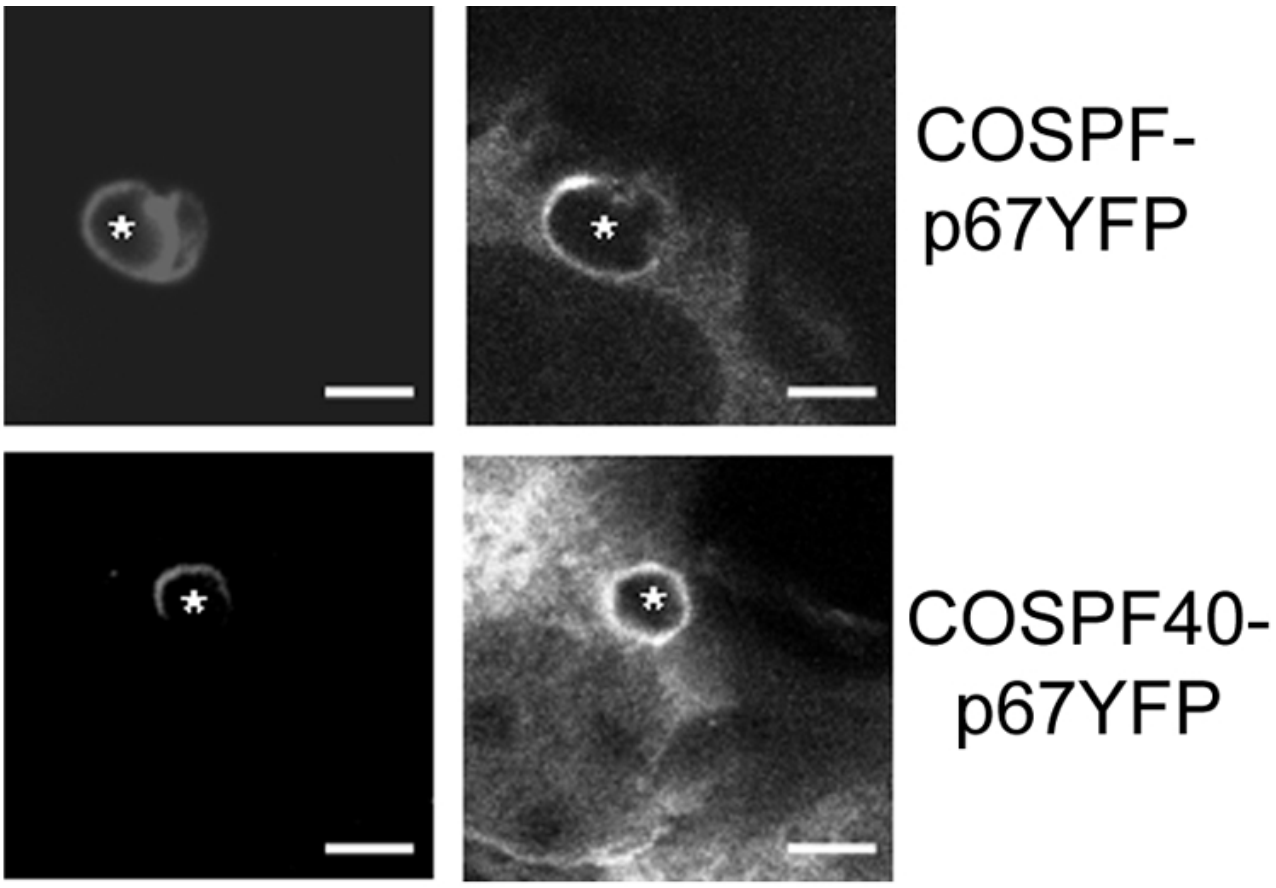
COSPF-
p67YFP
COSPF40-
p67YFP

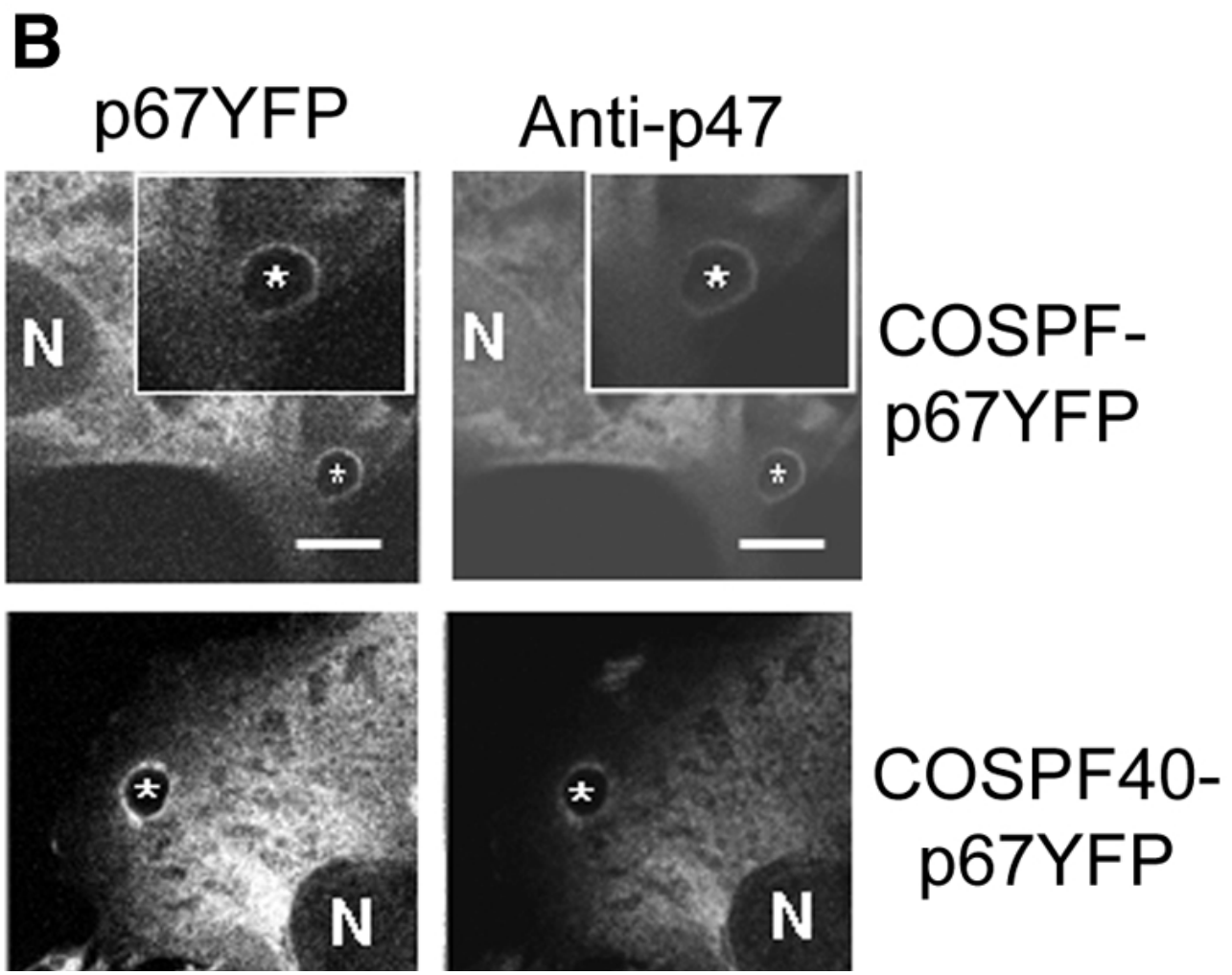
B
p67YFP
Anti-p47
N
N
COSPF-
p67YFP
N
N
COSPF40-
p67YFP

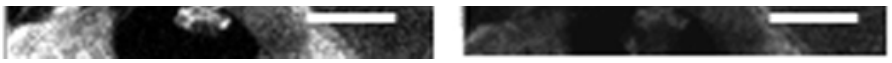

Translocation of p67^{phox}-YFP and p47^{phox} during phagocytosis of IgG-SRBCs by COS7 transgenic cells. IgG-SRBCs were fed to the indicated COS^{phox} cells growing on coverslip-bottomed dishes. N shows the location of nucleus and asterisks indicate the IgG-SRBC phagosomes. Bar represents 5 μm. (A) Images of Alexa-633–labeled IgG-SRBCs and p67^{phox}-YFP after fixation and analysis by confocal microscopy as described in "Immunofluorescence microscopy." (B) Simultaneous imaging of p67^{phox}-YFP and p47^{phox} after immunofluorescent staining with anti-p47^{phox} mAb and Alexa-555 goat anti–mouse IgG.

Figure 3

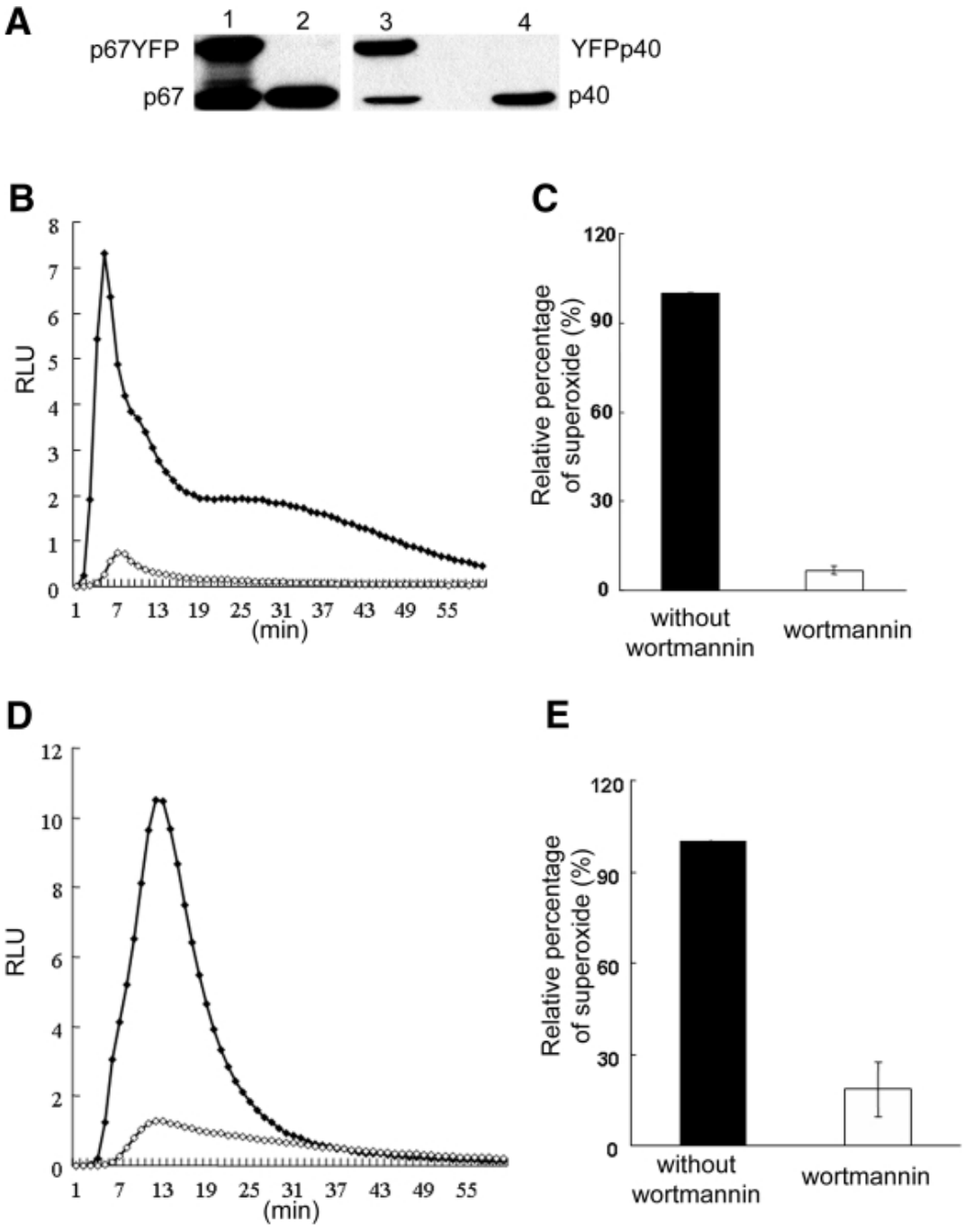

NADPH oxidase activity in neutrophil-differentiated PLB-985 cells expressing YFP-*phox* proteins during phagocytosis of IgG-zymosan. (A) Western blot analysis of exogenous YFP-tagged *phox* proteins and endogenous *phox* proteins in PLB-985 neutrophil lysates. Lane 1 shows PLB-p67YFP; lane 2, PLB-985; lane 3, PLB-YFPp40; and lane 4, PLB-985. (B-E) NADPH oxidase activity in PLB-p67YFP neutrophils

during synchronized phagocytosis of IgG-zymosan was quantified using isoluminol in the presence of HRP (B,C) to detect extracellular superoxide or luminol in the presence of SOD and catalase (D,E) to detect intracellular activity. Assays were performed in the absence or presence of preincubation with 100 nM wortmannin, as indicated. Representative kinetic plots (B,D) and mean plus or minus SD of relative integrated RLU data are shown (3 assays). The activity profile was similar for PLB-p67YFP and PLB-YFPp40 cells (data not shown). ♦ indicates no wortmannin; ◇, 100 nM wortmannin.

Figure 4

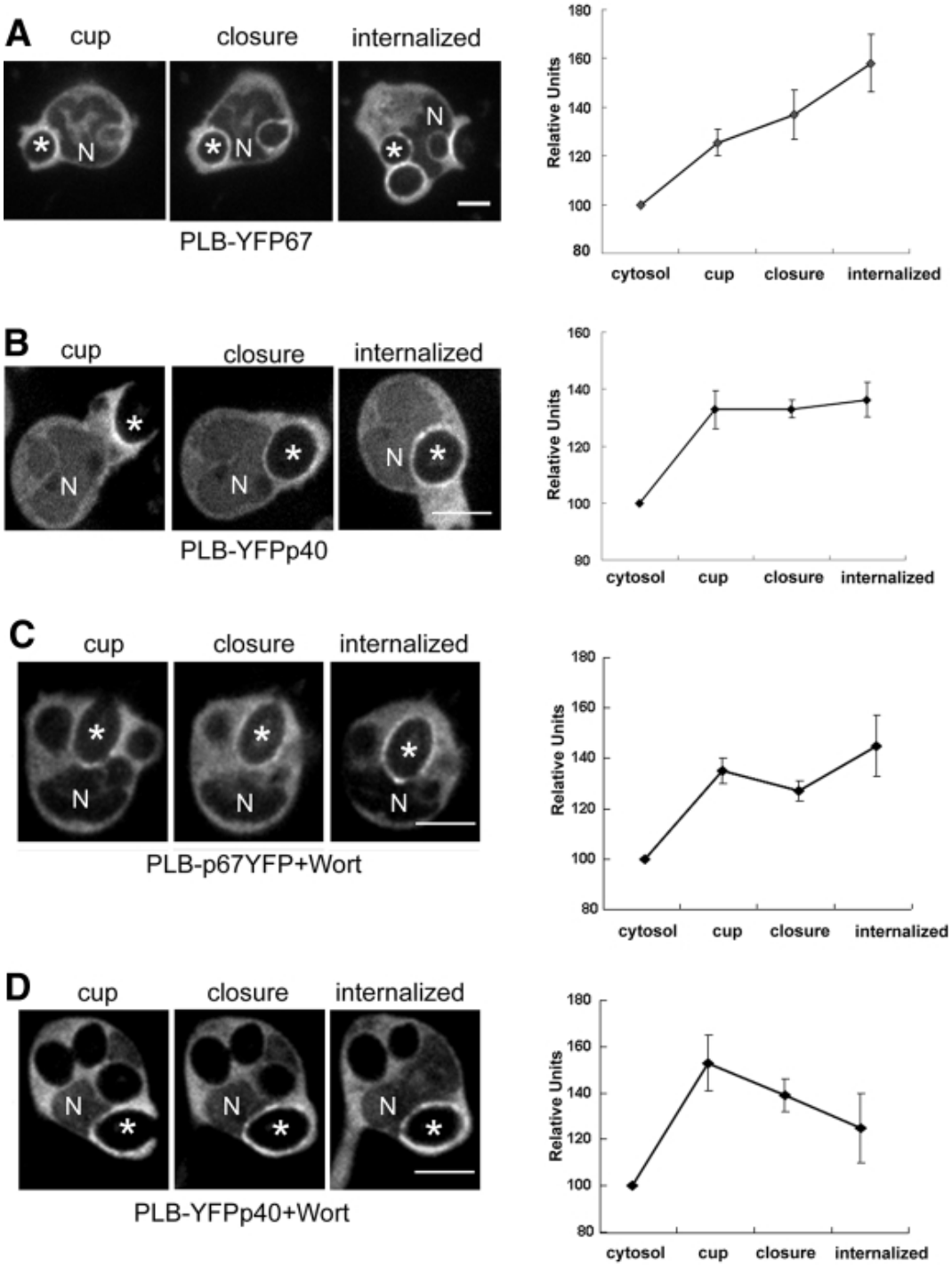

Translocation of YFP-tagged p67^{phox} and p40^{phox} during phagocytosis of IgG-zymosan in the presence and absence of wortmannin. Time-lapse confocal microscopy was used to monitor phagocytosis of IgG-zymosan by PLB-985 neutrophils expressing YFP-tagged p67^{phox} or p40^{phox} (Videos S1–S4). N shows the location of nucleus and asterisks indicate the IgG-zymosan phagosomes monitored. Bar represents 5 μm. (A,B) PLB-p67YFP and PLB-YFPp40 cells. The relative fluorescence intensity compared with the cytosol for 5

phagosomes at indicated stages is shown in the graphs, as mean plus or minus SE. Internalized indicates 200 or more seconds after phagosome closure. (C,D) PLB-p67YFP and PLB-YFPp40 neutrophils pretreated with 100 nM wortmannin before incubation with IgG-zymosan. N shows the location of nucleus and asterisks indicate the IgG-zymosan phagosomes monitored. Bar represents 5 μm. The relative fluorescence intensity compared with the cytosol for 5 to 7 phagosomes at indicated stages is shown in the graphs, as mean plus or minus SE. Internalized indicates 120 or more seconds after phagosome closure.

Figure 5

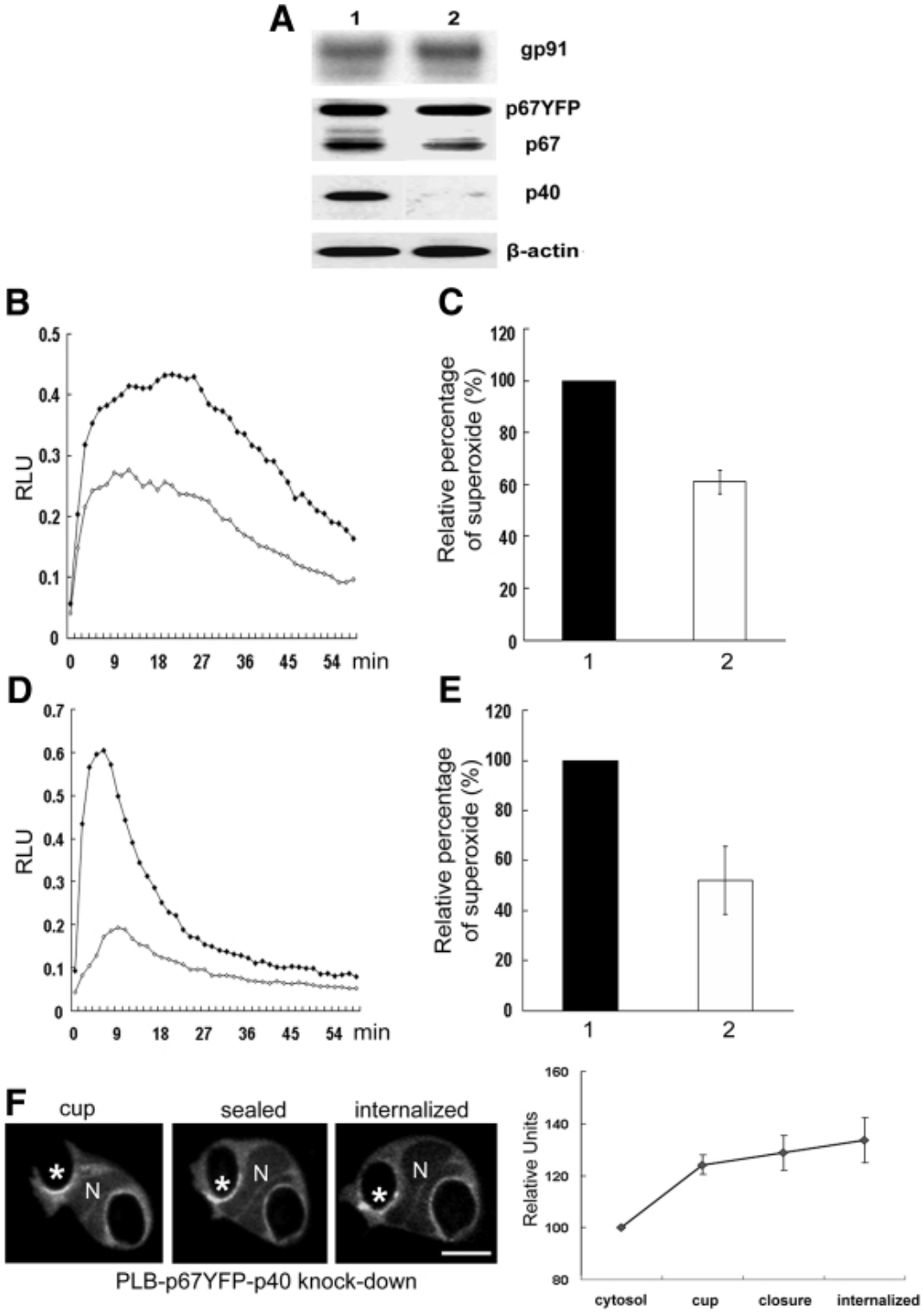

Effect of shRNA knockdown of p40^{phox} on NADPH oxidase activity in neutrophil-differentiated PLB-p67YFP cells. PLB-p67YFP cell lines induced for neutrophil differentiation were analyzed by Western

blot (A) for the expression of NADPH oxidase subunits and for NADPH oxidase activity during phagocytosis of IgG-zymosan (B-E). Lane 1 shows PLB-p67YFP-pSuper(neo) (empty vector) cells; lane 2, PLB-p67YFP $p40^{phox}$ knockdown cells. NADPH oxidase assays were performed using isoluminol in the presence of HRP (B,C) to detect extracellular superoxide or luminol in the presence of SOD (D,E) to detect intracellular activity. Representative kinetic plots (B,D) and mean plus or minus SD of relative integrated RLU data are shown (2 isoluminol assays and 4-6 luminol assays). ♦ indicates PLB-p67YFP; ◇, PLB-p67YFP with $p40^{phox}$ knockdown. (F) Time-lapse confocal images of $p67^{phox}$-YFP in $p40^{phox}$ knockdown cells (Video S5). The relative fluorescence intensity compared with the cytosol for 5 phagosomes at indicated stages is shown in the graph, as mean plus or minus SE. N shows the location of nucleus and asterisks indicate the IgG-zymosan phagosomes monitored. Bar represents 5 μm.

Figure 6

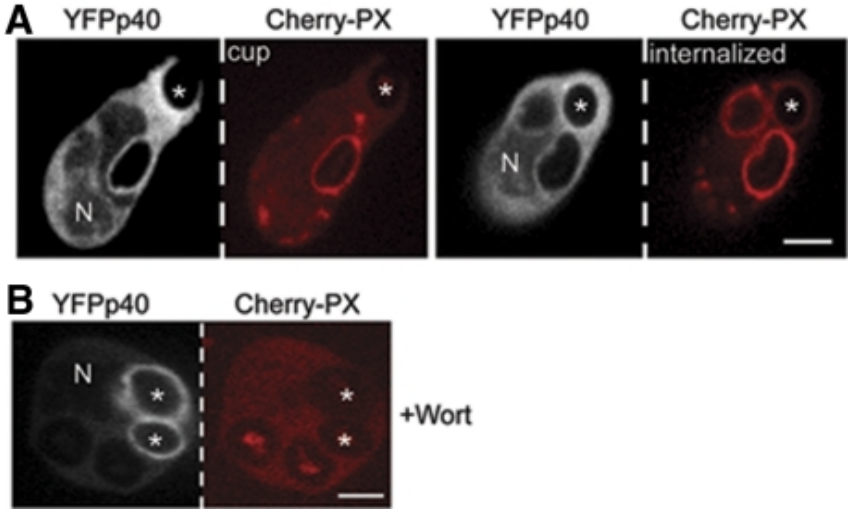

$p40^{phox}$ accumulates on to the phagosome independent of PI3P. Time-lapse confocal microscopy was used to monitor translocation of coexpressed YFP-$p40^{phox}$ and Cherry-PX_{40} in PLB-985 cells during phagocytosis of IgG-zymosan in the absence (A) and presence (B) of 100 nM wortmannin (Videos S6,S7). YFP-$p40^{phox}$ is detected on the cup, whereas Cherry-PX_{40} appears after closure (A). Cherry-PX_{40} does not accumulate in wortmannin-treated cells, although YFP-$p40^{phox}$ is present on internalized phagosomes (see also Figure 4D). N shows the location of nucleus in the YFP-$p40^{phox}$ panel. Phagosome stages are indicated and asterisks show the IgG-zymosan phagosomes monitored. Bar represents 5 μm.

Figure 7

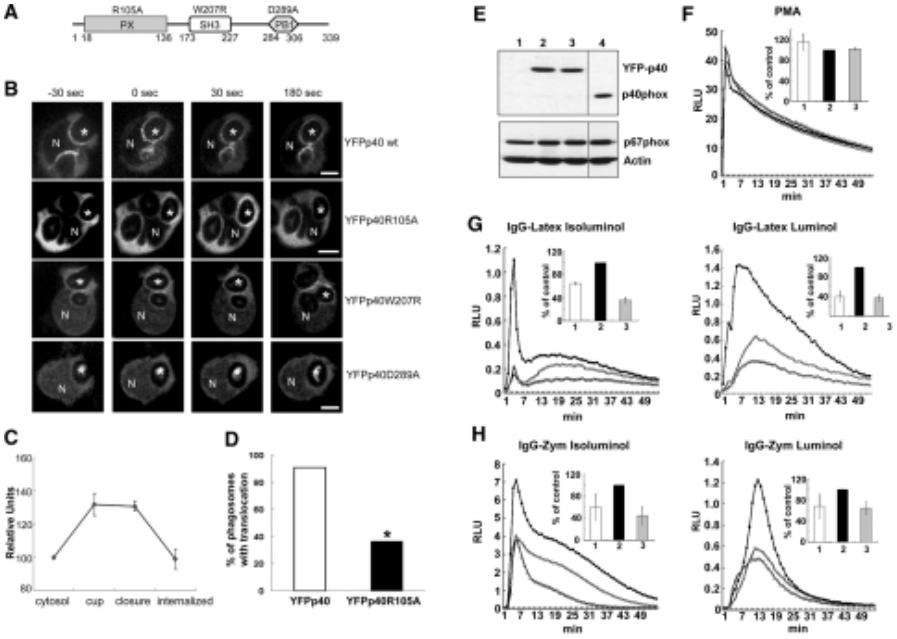

Effects of p40^{phox} mutations in the PX, SH3, and PB1 domains on translocation of p40^{phox} to the phagosome. (A) Schematic illustration of domains within p40^{phox} and mutants studied for translocation in PLB-985 neutrophils. (B) Time-lapse confocal microscopy was used to monitor translocation of wild-type YFP-p40^{phox} and indicated YFP-p40^{phox} mutants in PLB-985 neutrophils. In the experiments shown, all but YFP-p40^{phox}R105A were expressed using a transient transfection method. Wild-type YFP-p40^{phox}, YFP-p40^{phox}R105A, and YFP-p40^{phox}W207R accumulate on the phagosomal cup but YFP-p40^{phox}D289A does not. N shows the nucleus and asterisks indicate the IgG-zymosan phagosomes monitored. Bar represents 5 μm. (C) The relative fluorescence intensity compared with the cytosol for 5 phagosomes in PLB-YFPp40 R105A cells at indicated stages is shown in the graphs, as mean plus or minus SD. Internalized indicates 120 seconds after phagosome closure. (D) Phagosomes exhibiting translocation of either YFP-p40^{phox} or YPF-p40^{phox}R105A in the phagosomal cup were scored for persistence of translocation at 3 minutes after closure. The percentage of phagosomes showing persistent translocation of p40^{phox}R105A was significantly lower than for YPF-p40^{phox} ($*P < .03$, n = 11 phagosomes in each group; Fisher exact test). (E-H) A lentiviral vector expressing an shRNA from the 3′ untranslated region of the p40^{phox} cDNA was used to transduce PLB-985, PLB-YFPp40, or PLB-YFPp40R105A cells to generate p40^{phox} knockdown (p40KD PLB-985) cells deficient in endogenous p40^{phox}. (E) Western blot analysis of YFP-tagged proteins and endogenous p40^{phox}, p67^{phox}, and actin in PLB-985 neutrophil lysates. Lane 1 shows p40KD PLB-985; lane 2, p40KD PLB-YFPp40; lane 3, p40KD PLB-YFPp40R105A, and lane 4, PLB-985. A vertical line has been inserted to indicate a repositioned gel lane. (F-H) NADPH oxidase activity in neutrophil-differentiated p40KD PLB-985 cell lines. 1 or ◇ indicates p40KD PLB-985; 2 or ■, p40KD PLB-YFPp40; and 3 or ▵, p40KD PLB-YFPp40R105A. (F) PMA-induced superoxide release detected by isoluminol. The insert represents the mean plus or minus SD (total RLU value over 54 minutes, measured at 1-minute intervals) of 2 independent experiments. (G-H) Extracellular (isoluminol) and intracellular (luminol plus SOD and catalase) superoxide production during synchronized phagocytosis of IgG-Latex beads (G) or IgG-Zym (H). The insert represents the mean plus or minus SD (total RLU value over 54 minutes, measured at 1-minute intervals) of 3 independent experiments.